TiF_3 catalyzed MgH_2 as a Li/Na ion battery anode

Xu, Yaolin; Mulder, Fokko M.

DOI
10.1016/j.ijhydene.2018.09.003

Publication date
2018

Document Version
Accepted author manuscript

Published in
International Journal of Hydrogen Energy

TiF_3 catalyzed MgH_2 as a Li/Na ion battery anode

*Yaolin Xu, and Fokko M. Mulder**

Materials for Energy Conversion and Storage (MECS), Department of Chemical Engineering, Faculty of Applied Sciences, Delft University of Technology, Van der Maasweg 9, 2629 HZ Delft, The Netherlands

corresponding author: Fokko M. Mulder

E-mail: F.M.Mulder@tudelft.nl

Telephone/Fax: +31 15 27 85037

Keywords: Li ion battery, Na ion battery, MgH_2, TiF_3

Graphical abstract

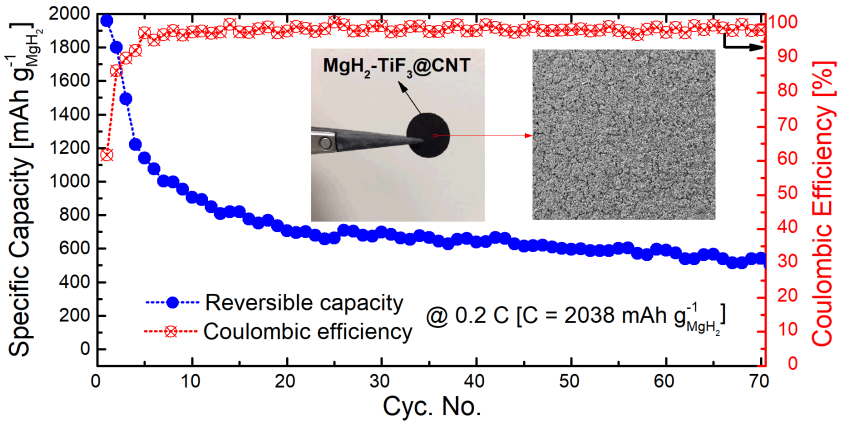

Abstract

MgH_2 has been considered as a potential anode material for Li ion batteries due to its low cost and high theoretical capacity. However, it suffers from low electronic conductivity and slow kinetics for hydrogen sorption at room temperature that result in poor reversibility, cycling stability and rate capability for Li ion storage. This work presents a MgH_2-TiF_3@CNT based Li ion battery anode manufactured via a conventional slurry based method. Working with a liquid electrolyte at room temperature, it achieves an high capacity retention of 543 mAh g^{-1} in 70 cycles at 0.2 C and an improved rate capability, thanks to the improved hydrogen sorption kinetics with the presence of catalytic TiF_3. Meanwhile, the first realization of Na ion uptake in MgH_2 has been evidenced in experiments.

1. Introduction

MgH_2 has been intensively researched as an active material for hydrogen storage due to its high capacity (7.6 w.t. %) and low cost [1,2]. It was introduced as a conversion anode material for reversible electrochemical Li ion uptake in 2008 [3], and has attracted growing research interest since then due to its high capacity for Li ion storage and cost-effectiveness [4-8]. Its lithiation undergoes dehydrogenation of MgH_2 with the formation of LiH (**Reaction 1**) resulting in a Li ion storage capacity of 2038 mAh g^{-1}, which is defined as the theoretical capacity. Li-Mg alloying (**Reaction 2**) takes place when further lithiation proceeds and the achieved capacity can be even higher.

$$2\ Li + MgH_2 \rightarrow Mg + 2\ LiH \quad (1)$$

$$x\ Li + y\ Mg \rightarrow Li_xMg_y \quad (2)$$

However, despite its high capacity, MgH_2 faces tremendous challenges in reaching its potential in Li ion batteries. The most critical issue is the limited H mobility in MgH_2 at room temperature and thus sluggish kinetics for Li ion uptake. Considerable research efforts have been made, among which the utilization of MgH_2 in solid state Li ion batteries has achieved significant progress [8-14]. For instance, a (Nb_2O_5-doped MgH_2)-$LiBH_4$-acetylene black (4:3:3 in mass) composite achieved a capacity retention of 700 mAh g^{-1} in 100 cycles at 120 ℃ [8]. However, the functionality of these solid state batteries entails a high operating temperature (above 100 ℃) [8-13], and catalysts (e.g. Al_2O_3 [9] and Nb_2O_5 [8, 10-12]) and a substantial amount of $LiBH_4$ [8, 11-14] are required to improve H mobility and Li ion diffusivity. The high operational temperature largely limits its potential for practical applications and the addition of large amount of H conducting but storage-inactive $LiBH_4$ also reduces the overall capacity of the electrode and cost-effectiveness. Very recently, El kharbachi *et al.* has demonstrated the possibility of a MgH_2 anode based solid state lithium battery operating at room temperature by embedding nanosized MgH_2 in a novel Li_2S-P_2S_5-

$Li(BH_4)_{0.75}I_{0.25}$ based solid electrolyte, but the reversibility and cycling stability has to be greatly improved [14]. Therefore, the research on MgH_2 based solid state batteries is out of the scope of our work.

Intensive research on MgH_2 anodes have also been carried out for room-temperature liquid-electrolyte-based Li ion batteries in recent years [3,15-19], and the solutions to improve the kinetic properties include nanosizing MgH_2 [3,15,16], producing more cyclable β-MgH_2 through gas phase hydrogenation of Mg [17-19], and incorporating a secondary hydride phase (e.g. TiH_2) [17,18]. Moreover, both MgH_2 and its lithiation product, LiH, are electrically insulating, and the uptake of Li ions in MgH_2 is also accompanied with a large volume change (up to 85%), therefore a large content of advanced carbon and binders appear to be necessary to maintain the electrical conduction and structural integrity of the electrode during cycling. For instance, a composite of ultra-small (~ 5 nm) MgH_2 embedded within a high surface area graphite matrix (MgH_2 : C = 1:1 in mass), synthesized with a bottom-up approach, showed a retained capacity of around 500 mAh g^{-1} for Li ion storage after 20 cycles [16]. A composite of nanostructured MgH_2, carboxymethyl cellulose formate (CMC-f) binder and preground $C_{t,x}$ carbon (MgH_2 : CMC-f : $C_{t,x}$ = 1:1:1 in mass) reached a capacity retention of 542 mAh g^{-1} in 40 cycles [19].

However, in the above-mentioned studies, besides the limited commercial viability due to the complex synthesis and/or high material cost, the kinetic properties of Li ion transport were still limited, and the cycling rates were extremely low (usually 0.1 Li per hour, i.e. 0.05 C with C = 2038 mA g^{-1}) limited by the sluggish ionic transport. As a result, the reversibility of Li ion storage was rather low, leading to a poor cycling stability and rate capability. Moreover, in experimental studies, mechanically pressed disc-like MgH_2 electrodes were commonly prepared for the electrochemistry measurement. In such electrodes the Li ion diffusion kinetics throughout the electrode is limited because the pellet should remain intact, which is a

further handicap for sustained cycling stability and high rate capability. Recently, a magnetron-sputtered MgH_2-C thin-film anode (~270 nm) with Pd coating has also been reported, however, its active mass loading is extremely low (< 0.1 mg cm^{-2}), and the electrode is non-porous resulting in limited Li ion diffusion in the solid and poor cycle life (10 cycles) [20]. Recently El kharbachi *et al.* has introduced the conventional slurry-based method to produce porous, thin-film MgH_2 electrodes using N-Methyl-2-pyrrolidone (NMP) as a solvent, but the cycling performance is still to be improved due to the aggregation issue of MgH_2 that limits both the electronic and ionic transport [21]. Furthermore, the formation of solid electrolyte interphase (SEI) is unavoidable in organic liquid electrolyte based Li ion batteries. The SEI layer is mechanically unstable, and therefore continuous SEI growth occurs during cycling resulting in the loss of active materials and capacity decay. This issue is even aggravated taking into account the pulverization of active materials caused by the large volume expansion/contraction during de-/lithiation.

In this work, we present a MgH_2-TiF_3@carbon nanotubes (CNT) composite based Li ion battery anode, fabricated through a slurry-based approach using anhydrous tetrahydrofuran (THF), which has a lower boiling point (66 °C, compared to 202 °C for NMP) and is thus easier to be removed, as a solvent. 5 mol. % TiF_3 is present in the composite as a catalyst to enhance the kinetics for hydrogen sorption and Li ion uptake in MgH_2. Transitional metal halides (e.g. TiF_4 [22], $ZrCl_4$ [23] and NbF_5 [24]) have been proven to be able to improve the hydrogen sorption kinetics in MgH_2; and it has been shown by some of us that, in gas phase experiments, the hydrogen absorption/release is possible at reduced temperatures with the catalysis of TiF_3 [25]. The role of CNT in the composite is to address the poor electronic conductivity of MgH_2 and LiH, providing sufficient electronic charge transport throughout the electrode and enabling its electrochemical function. Furthermore, to suppress the SEI growth, 10 w.t. % fluoroethylene carbonate (FEC) was utilized as an electrolyte additive. The MgH_2-

TiF_3@CNT anode exhibits a capacity retention of 543 mAh g^{-1} in 70 cycles at 0.2 C and outstanding rate capability in liquid electrolyte based Li ion batteries . Meanwhile, this work has, for the first time, experimentally achieved Na ion uptake in a MgH_2 based electrode.

2. Experimental details

Sample Preparation: MgH_2 (hydrogen-storage grade, Aldrich) was mixed with 5 mol. % TiF_3 (Alfa Aesar) and CNT (industrial standard, 150 – 210 m^2 g^{-1}) (MgH_2-TiF_3 : CNT = 3:1 in mass), and subsequently was ball milled with a Fritsch Planetary Mono Mill PULVERISETTE 6 for 50 hours at 400 rpm under Ar atmosphere using a Tungsten Carbide grinding bowl and a ball-to-powder mass ratio of 50:1.

Characterization: The micro-morphology of MgH_2-TiF_3@CNT and the as-prepared electrode were imaged with a JEOL JSM 6010F scanning electron microscope working at 5 kV. XRD measurements were performed with a PANalytical X'Pert Pro PW3040/60 diffractometer (Cu K_α radiation) operating at 45 kV and 40 mA. The lithiated electrode for XRD measurement was washed 3 times with diethyl carbonate (DEC) to remove soluble electrolyte residuals in the electrode, and were dried in a glovebox before the measurements.

Electrode preparation and battery assembly: The MgH_2 based Li ion battery anodes were prepared inside an Ar-filled glovebox using a conventional slurry based method using anhydrous THF (≥ 99.9%, Sigma-Aldrich) as the solvent. and polyvinylidene difluoride (PVDF, Kynar flex) worked as the binder and super P carbon black (TIMCAL) was used to integrate the electrical conduction throughout the electrode. The slurry (MgH_2-TiF_3@CNT: super P carbon black : PVDF = 70:15:15 in mass) was casted on a planar Cu foil (12.5 μm, Goodfellow) with a doctor blade and dried inside the glovebox. The thickness of active materials was ~ 20 μm and the mass loading was ~ 0.5 mg cm^{-2}. The composition/preparation of the MgH_2 based Na ion battery anodes was similar to that of the Li ion batteries except that

super P carbon black instead of CNT was utilized as the conducting additive in the ball milled composite.

Half-cell Li/Na ion batteries were assembled inside an Ar-atmosphere glovebox with the O_2 and H_2O levels < 0.1 ppm. A Li/Na foil (Aldrich) was applied as the counter electrode. The working electrolyte for Li ion batteries was 1 M $LiPF_6$ dissolved in ethylene carbonate (EC), DEC and FEC (EC : DEC = 1:1 in volume with 10 % FEC); and 1 M $NaPF_6$ dissolved in EC and dimethyl carbonate (DMC) and (EC : DMC = 1:1) was applied as the electrolyte in Na ion batteries. A borosilicate glass micro fibre (Whatman) was used as the separator.

Electrochemistry measurements: The galvanostatic electrochemical properties were tested with a MACCOR 4600 battery cycler. The cut-off voltages for Li ion batteries were 0.005 V and 3.0 V *versus* Li/Li^+ for discharge and charge, respectively. The cycling voltage range for Na ion batteries was 0.005 – 2.8 V *versus* Na/Na^+, and the cyclic voltammograms were obtained with an Autolab potentiostat scanning within the same voltage range.

Subtraction of the carbon capacity: The specific capacities reported in this paper were calculated based on the mass of MgH_2 (*excl.* carbon additives). The capacity of CNT was determined by measuring its electrochemical performance (**Fig. S1**) in Li ion batteries; and the capacity of super P carbon black has been determined by us in previous work [26]. The capacity contributions from these carbon additives were then subtracted to obtain the specific capacity of MgH_2.

3. Results and discussions

X-ray Diffraction (XRD) patterns of the MgH_2-TiF_3@CNT composite (**Fig. 1a**) show the characteristic diffraction peaks of MgH_2 (110), (101), (200) and (211) lattice planes at 27.7°, 35.6°, 39.6°and 54.4°, respectively. Weak but distinguishable peaks of TiF_3 are present at 23.1°, 31.4°, 41.0° and 48.3°. The peaks at 25.6°, 42.7° and 78.2° can be allocated to the

Bragg reflections on CNT [27-28] The average crystalline domain size of MgH_2 is ~ 10 nm calculated based on the line shape of MgH_2 in the Rietveld refinement (**Fig. S2**). The scanning electron microscopy (SEM) images of the sample (**Fig. 1b – 1d**) show aggregates of sub-micro grains induced by the high energy ball milling. Energy-dispersive X-ray spectroscopy (EDX) (**Fig. S3**) demonstrates that the distribution of TiF_3 next to MgH_2 is homogeneous on the basis of the superposition of Mg and F element distribution at the submicro-/nanoscale. The nature of the small grains is thus the agglomeration of nanosized MgH_2 and TiF_3 which warrants an optimal catalytic activity of TiF_3.

Morphological images of the as-prepared electrode (**Fig. 1e – 1f** & **S4**) show that the active material loading is uniform with micro-/nanoscale porosities all over the electrode, and the active material grains are integrated by the binder and carbon matrix. The porous nature of the electrode allows the access of liquid electrolyte throughout the electrode and reduces the Li ion diffusion pathway through the solid phase fractions.

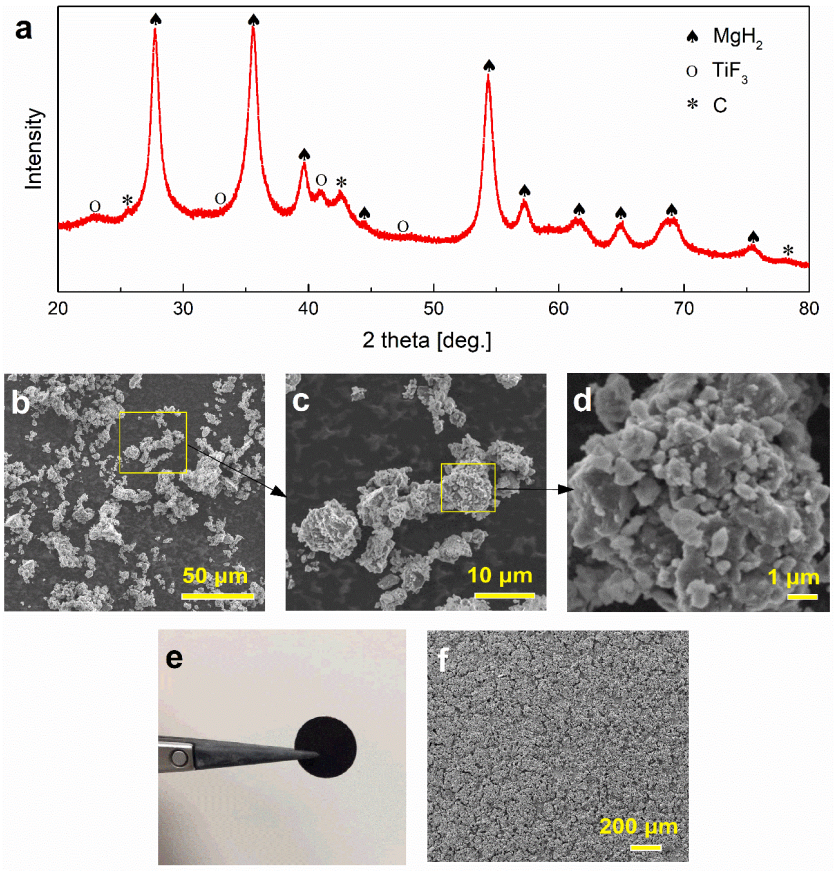

Fig. 1. (a), XRD patterns of the ball-milled MgH_2-TiF_3@CNT sample. (b) – (d), SEM images of the sample at different magnifications. (e), a photo and (f), a SEM image of the as-prepared electrode (12.7 mm in diameter).

The electrochemical performance of the MgH_2 based anodes was measured within half-cell Li ion batteries. **Fig. 2a** shows that, cycling at 0.2 C, a capacity of 3254 mAh g^{-1} was achieved for the first lithiation, and the following delithiation reaches a capacity of 1959 mAh g^{-1}. This relatively low Coulombic efficiency (61.7 %) mainly originates from the irreversible SEI formation. The reversible capacity declines during the first few cycles and 1139 mAh g^{-1} is retained after 5 cycles. The Coulombic efficiency increases to 86.3 % and 97.4 % at the 2^{nd} and 5^{th} cycle, respectively, indicating that though further SEI growth still takes place but the amount is increasingly limited, and most of the Li ions absorbed during lithiation can be released during the following delithiation. It also indicates that the increasingly reduced capacity during Li ion uptake is the main reason of the rapidly decaying reversible capacity retention. The capacity retention slips to 707 mAh g^{-1} after 20 cycles, and reaches 543 mAh g^{-1} in 70 cycles. **Fig. 2b** shows that the initial reversible capacity for Li ion storage amounts to 2293, 2291 and 824 mAh g^{-1} at 0.05, 0.1 and 0.5 C, respectively. Compared with the published results on MgH_2 based anode cycling in liquid electrolytes [5,6,8,17], the MgH_2-TiF_3@CNT electrode in this work exhibits improved rate capability. Such improved kinetics supports that TiF_3 is an effective catalyst for hydrogen absorption and release in Mg/MgH_2.

The initial Li ion uptake (**Fig. 2c**) shows a voltage plateau at ~ 1.2 V corresponding to the SEI formation, which is not observed in the following cycles, and a lithiation capacity of around 200 mAh g^{-1} is reached during this process. The main lithiation of MgH_2 takes place at a lower voltage range including two stages: (i), a voltage plateau at ~ 0.2 V related to the hydrogen extraction from MgH_2 with the formation of LiH (**Reaction 1**); and (ii), a low voltage plateau ~ 0.05 V associated with the alloying process between Mg and Li (**Reaction**

2). At the beginning of the first stage, the voltage undergoes a dip to 0.13 V, which is consistent with the other studies [3,15-17], possibly originating from the large energy barrier of initial LiH nucleation on the surface of Mg, before it rises to the main voltage plateau at ~ 0.2 V due to the co-existence of Mg and MgH_2. Upon the complete depletion of MgH_2, the presence of a single MgH_2 phase results in a declining voltage slope. When the voltage goes down to 0.08 V the cumulative lithiation capacity reaches above 2150 mAh g^{-1} indicating that the Li ion uptake in MgH_2 achieves a capacity of ~ 1950 mAh g^{-1}, which is close to the theoretical capacity. In the second stage, the voltage also exhibits a plateau originating from the co-existence of Li and Mg solid solutions and a following sloped voltage attributed to one single phase (Li solid solution) [3,15]. The cumulative lithiation capacity reaches ~ 3250 mAh g^{-1} when the cut-off voltage is reached revealing a Li ion storage capacity of ~ 1100 mAh g^{-1} (i.e. Li : Mg ≈ 1 : 1) in the alloying reaction. In the following delithiation, the voltage exhibits a reverse course of lithiation. It begins with a de-alloying process from Li_xMg_y that occurs at a voltage range < 0.25 V achieving a capacity of about 600 mAh g^{-1}. Subsequently, it undergoes a plateau at ~ 0.6 V associated with the delithiation from LiH and the hydrogenation of Mg, which obtains a capacity of ~ 1400 mAh g^{-1}. The Coulombic efficiency (72 %) of the delithiation from LiH is higher than that of the de-alloying process (55 %), indicating that the Li ion extraction from the Li-Mg alloys is less reversible and may cause the active material loss and capacity deterioration over cycling.

The overpotential between the Li-Mg de-alloying and alloying is less than 0.2 V; while it rises up to 0.5 V between the lithiation of MgH_2 (forming Mg) and the reverse reaction. This overpotential increase stems from the significant conductivity reduction from conductive metallic Mg to electrically insulating MgH_2. Over cycling, the voltage plateaus become increasingly sloped with growing overpotentials, which results from the build-up of internal resistance due to the gradual structural deformation over repetitive volume expansion and

contraction. As a result, the lithiation cut-off voltage has been reached earlier and before the Li-Mg alloying occurs, therefore, the achieved lithiation capacity drops. Given that the low lithiation capacity is the main limiting factor for the reversible capacity retention as explained before, we can conclude that the drastic capacity drop within the first few cycles mainly originates from the increasing overpotential resulting in the decreasing amount of Li ion uptake during lithiation.

The voltage profiles at different current rates (**Fig. 2d**) show growing overpotentials when the current rate increases. It leads to a more rapid voltage collapse to the cut-off voltage and thus a lower capacity when it is lithiated at a higher current rate; and hence in the following Li ion extraction step, the achieved capacity is lower. It is also observed that the Li-Mg alloying reaction (near 0 V) reduces significantly as the overpotential grows.

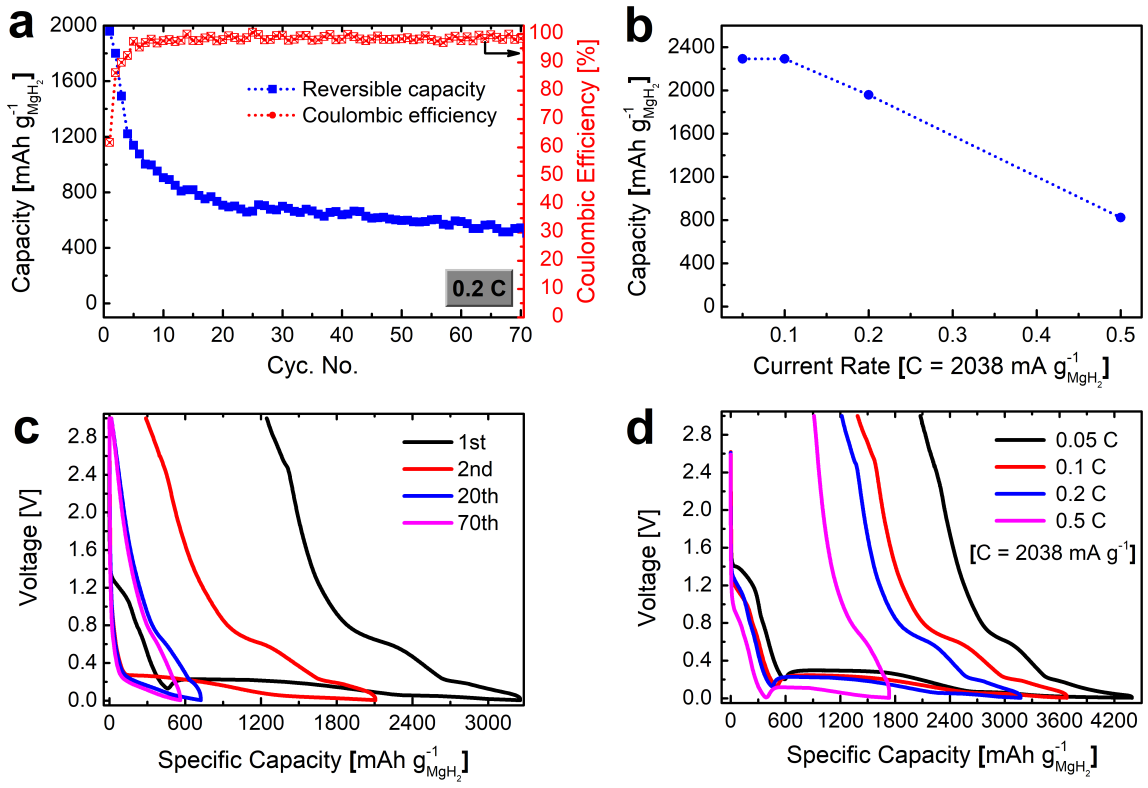

Fig. 2. (a), The capacity retention and Coulombic efficiency at 0.2 C (C = 2038 mA g^{-1}). (b), The initial reversible capacity of the MgH_2-TiF_3 anode at different C-rates. (c), Voltage

profiles of the 1st, 2nd, 20th and 70th cycles of the MgH_2-TiF_3 anode at 0.2 C. (d), Voltage profiles of the MgH_2-TiF_3 anode for the 1st cycle at different C-rates.

The high performance of the MgH_2-TiF_3@CNT based Li ion battery anode may benefit from the synergistic effects of several factors. Firstly, the slurry-casting manufactured electrode, compared with a pellet electrode, is more porous and allows a facile access for the liquid electrolyte to the active materials and may enable faster Li ion transport throughout the electrode. Therefore, a lower internal ionic resistance is expected resulting in a lower overpotential, and the rate capability could be promoted as well. Moreover, the voids in the electrode can accommodate the volume change upon Li ion insertion. Secondly, the active material grains are embedded within the CNT matrix warranting intimate electronic conduction between the active materials and the carbon network induced by high energy ball milling, and enabling sustained electrical conduction between the grains over cycling. Thirdly, The FEC additive in the electrolyte induces a thin, stable and compact LiF-dominant SEI layer that prevents further SEI growth, and therefore an enhanced Coulombic efficiency and cycling stability can be achieved [29-31]. This is also evidenced by comparing with the results with a FEC-free electrolyte (**Fig. S5c**). Last but not least, the catalytic TiF_3 accelerates the hydrogen sorption kinetics in MgH_2 and leads to facilitated lithium ion uptake. Specifically, during the initial lithiation, apart from the dehydrogenation of MgH_2 (**Reaction 1**), the presence of TiF_3 next to MgH_2 leads to the (irreversible) formation of MgF_2 and TiH_2 (**Reaction 3**). Subsequently, the small MgF_2 crystallites act as a grain refiner (i.e. seed crystals for the growth of MgH_2) for MgH_2/Mg, keeping their crystallites small [25,32]. This grain refinement mechanism results in a destabilized system facilitating the hydrogen sorption of Mg/MgH_2, and in this way the Li ion uptake is also accelerated.. Meanwhile, TiH_2 may also be lithiated (**Reaction 4**) and vanishes, but it is much more difficult since the enthalpy of

formation of TiH_2 (− 136 kJ mol^{-1}) is more negative than MgH_2 (− 74 kJ mol^{-1}) and there is no alloying between Li and Ti [33].

$$2\ Li + 3\ MgH_2 + 2\ TiF_3 \rightarrow 3\ MgF_2 + 2\ TiH_2 + 2\ LiH \qquad (3)$$

$$2\ Li + TiH_2 \rightarrow Ti + 2\ LiH \qquad (4)$$

The advantageous catalytic effect is also evidenced by measuring the performance of a TiF_3-free electrode at the same conditions as the MgH_2-TiF_3 electrode (**Fig. S5c**). Recently such grain refinement has been employed as well in Li-O_2 electrode systems [34].

To further investigate the behaviours of TiF_3 and MgH_2 during cycling, XRD patterns of a MgH_2-TiF_3@CNT electrode (**Fig. 3**) were acquired at different stages: pristine, lithiated to 0.05 V and 0.005 V, respectively, at 0.1 C. In the pristine electrode, apart from the peaks from MgH_2, the main diffraction peaks of TiF_3 are weak but distinctively recognizable. Bragg diffractions on the CNT are visible as well. When it is lithiated to 0.05 V, MgH_2 disappears while Mg and LiH show up, and the Li-Mg alloy emerges as well. It indicates that the dehydrogenation of MgH_2 (**Reaction 1**) is accomplished and the lithiation has proceeded to the Mg-Li alloying (**Reaction 2**). It is also observed that TiF_3 vanishes due to **Reaction 3**, but the peaks of MgF_2 and TiH_2 are hardly visible due to their much lower presence together with much smaller grain sizes (~ 3 nm) compared with MgH_2/Mg (~ 10 nm) based on the Rietveld refinement (**Fig. S6** & **Table S1 – S2**), and the peak broadening is significant in the XRD signals. These findings are in good agreement with the previous studies [25,32]. During the further lithiation till 0.005 V, LiH remains unaffected while Mg alloys with Li forming Li_xMg_y; the stoichiometry is $x : y \approx 1 : 1$, and the average alloy grain size amounts to 18.3 nm (**Table S3**) The grain size growth from Mg (10.1 nm) to Li_xMg_y (18.3 nm) originates from the absorption of Li ions in the Mg structure. The Rietveld refinement also indicates the crystal structure transformation from a hexagonal lattice (Mg, space group: *p63/mmc*) to cubic (Li_xMg_y, space group: *Im-3m*) upon Li ion uptake. Moreover, the larger size of Li_xMg_y

compared to LiH (< 8 nm) results in a slower Li ion desorption and thus worse reversibility. This is also consistent with the higher Coulombic efficiency of Li ion extraction from LiH compared to the dealloying of intermetallic Li_xMg_y (as discussed in **Fig. 2c)**.

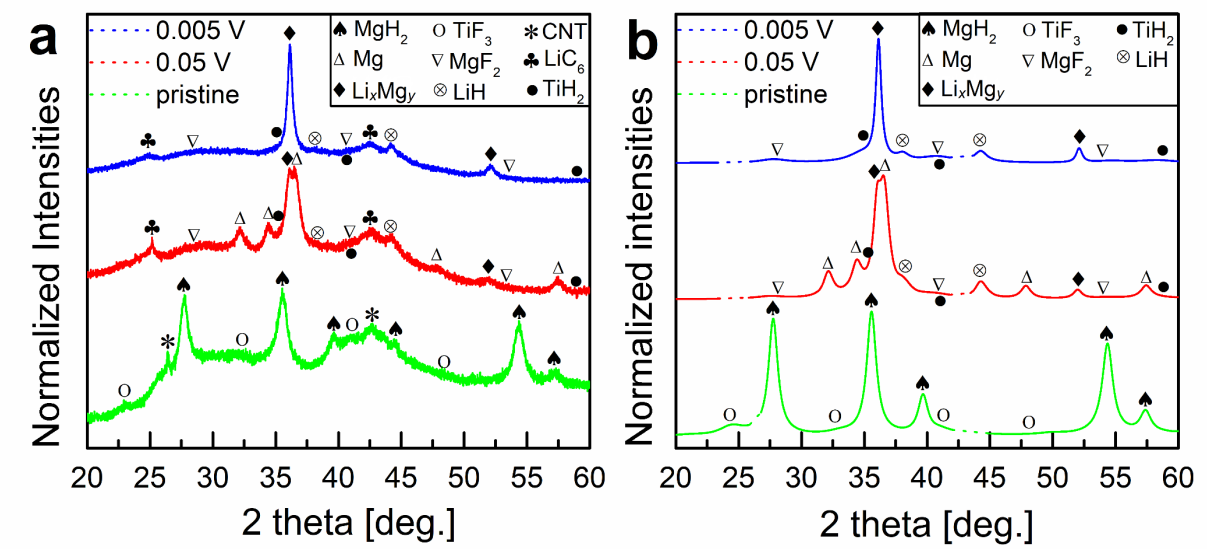

Fig. 3. XRD patterns of the MgH_2 electrode at different stages: pristine, lithiated to 0.05 V and 0.005 V, respectively. (a), experimental data; (b), Refined XRD patterns after subtraction of background; (The 2 theta ranges of carbon and Li-C alloy has been subtracted since it is out of the scope of this work. Details on the refinement are displayed in **Fig. S6**.) Here the electrode is a pressed pellet (~ 70 μm in thickness), instead of a slurry based electrode, in order to avoid the strong Bragg reflections from the Cu current collector and to produce XRD patterns with a higher signal-to-noise ratio.

The promising results of the TiF_3 catalyzed MgH_2 anode in Li ion batteries encourage us to investigate its potential for Na ion batteries. Though a sodiation voltage has been predicted theoretically [35,36], MgH_2, or any other metal hydride, has not been reported to have a capability of Na ion storage probably due to the poor kinetics of Na ion transport. The improved kinetics of Li ion uptake in the TiF_3 catalyzed MgH_2 suggests that the Na ion diffusion may be facilitated with the catalytic TiF_3 and thus enable the realization of Na ion uptake in MgH_2.

In this work, the possibility of Na ion insertion in MgH_2 was studied by testing MgH_2 based anodes within Na ion half-cells. The experimental result illustrates that, judging from the comparison of voltage profiles between the MgH_2 based electrode (**Fig. 4a**) and the carbon additive based electrode (**Fig. S7a**), the voltage plateau at 0.15 V and part of the sloping voltage between 0.15 V and the sodiation cut-off voltage originate from the sodiation of MgH_2, and the achieved capacity in this process is only ~ 350 mAh g^{-1}; during desodiation, the sloping voltage range of 0.4 – 0.9 V may be partially related to the Na ion extraction from the product of sodiated MgH_2 achieving a capacity of merely ~ 80 mAh g^{-1} (*excl.* the capacity contribution from the carbon additive [26]). Although the achieved capacity is low, the realization of Na ion insertion in MgH_2 is evident. It is also evidenced by the cyclic voltammograms (**Fig. 4b** & **S7b**) and XRD patterns of the sodiated MgH_2 electrode (**Fig. S8**).

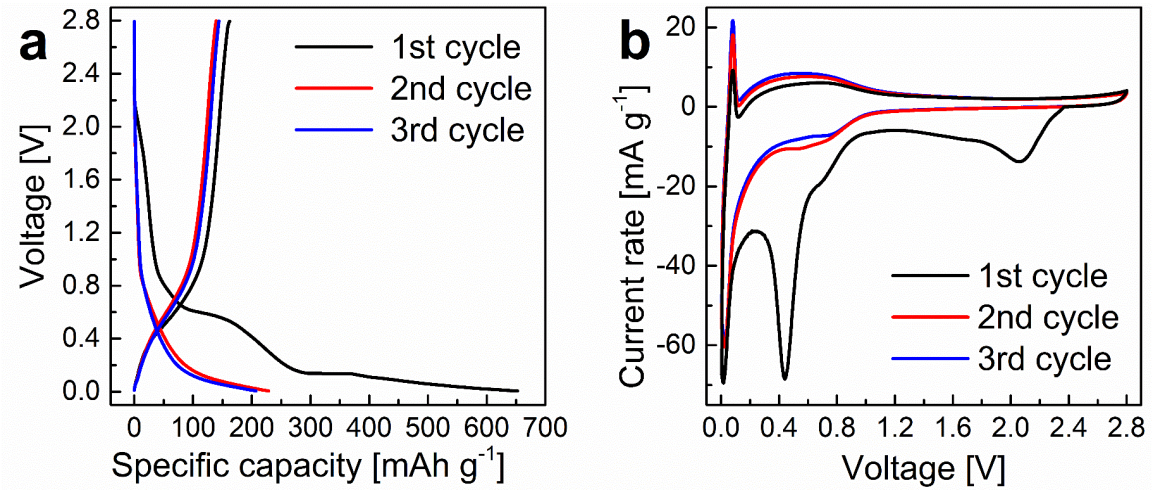

Fig. 4. (a), Voltage profiles at 0.05 C and (b), Cyclic voltammograms (scan rate: 0.02 mV s^{-1}) of the MgH_2-TiF_3 electrode tested in a Na ion half-cell.

4. Conclusions

This work presents a novel MgH_2-TiF_3@CNT composite based anode which achieves promising electrochemical performance in liquid electrolyte based Li ion batteries. *MgF_2 derived from the TiF_3 during the initial lithiation process work as the catalytic species to*

improve the electrochemical hydrogen sorption f Mg/MgH_2 and therefore to facilitate the Li ion uptake in MgH_2. We also find out that the dealloying of intermetallic Li-Mg is less reversible than the delithiation of LiH due to its larger grain size. Moreover, Na ion uptake in the MgH_2-TiF_3 electrode has been, for the first time, witnessed in experiments even though the cycling performance is poor and the reaction mechanism is still to be elucidated. It may stimulate considerable follow-up research on metal hydrides for reversible Li/Na ion uptake.

Acknowledgements

This work is supported by A green Deal in Energy Materials (ADEM) grant funded by Dutch Ministry of Economic Affairs and ADEM industrial partners.

Declarations of interest

None.

Appendix A. Supplementary data

Supplementary information related to this article can be found at *[XXXXXXXXX]*.

References

[1] Schlapbach L, Zuttel A. Hydrogen-storage materials for mobile applications. Nature. 2001;414:353-8.

[2] Züttel A. Materials for hydrogen storage. Mater Today. 2003;6:24-33.

[3] Oumellal Y, Rougier A, Nazri GA, Tarascon JM, Aymard L. Metal hydrides for lithium-ion batteries. Nat Mater. 2008;7:916-21.

[4] Brutti S, Meggiolaro D, Paolone A, Reale P. Magnesium hydride as negative electrode active material in lithium cells: A review. Mater Today Energy. 2017;3:53-9.

[5] Sartori S, Cuevas F, Latroche M. Metal hydrides used as negative electrode materials for Li-ion batteries. Appl Phys A: Mater Sci Process. 2016;122:1-7.

[6] Aymard L, Oumellal Y, Bonnet J-P. Metal hydrides: an innovative and challenging conversion reaction anode for lithium-ion batteries. Beilstein J Nanotechnol. 2015;6:1821-39.

[7] Brutti S, Panero S, Paolone A, Gatto S, Meggiolaro D, Vitucci MF, et al. Hydrides as High Capacity Anodes in Lithium Cells: An Italian “Futuro in Ricerca di Base FIRB-2010” Project. Challenges. 2017;8.

[8] Zeng L, Kawahito K, Ichikawa T. Metal hydride-based materials as negative electrode for all- solid-state Lithium-ion batteries. In: Yang D, editor. Alkali-ion Batteries. Rijeka: InTech; 2016, p. 75-91.

[9] Ikeda S, Ichikawa T, Goshome K, Yamaguchi S, Miyaoka H, Kojima Y. Anode properties of Al_2O_3-added MgH_2 for all-solid-state lithium-ion batteries. J Solid State Electrochem. 2015;19:3639-44.

[10] Ikeda S, Ichikawa T, Kawahito K, Hirabayashi K, Miyaoka H, Kojima Y. Anode properties of magnesium hydride catalyzed with niobium oxide for an all solid-state lithium-ion battery. Chem Commun. 2013;49:7174-6.

[11] Zeng L, Kawahito K, Ikeda S, Ichikawa T, Miyaoka H, Kojima Y. Metal hydride-based materials towards high performance negative electrodes for all-solid-state lithium-ion batteries. Chem Commun. 2015;51:9773-6.

[12] Zeng L, Ichikawa T, Kawahito K, Miyaoka H, Kojima Y. Bulk-type all-solid-state Lithium-ion batteries: remarkable performances of a carbon nanofiber-supported MgH_2 composite electrode. ACS Appl Mater Interfaces. 2017;9:2261-6.

[13] López-Aranguren P, Berti N, Dao AH, Zhang J, Cuevas F, Latroche M, et al. An all-solid-state metal hydride – Sulfur lithium-ion battery. J Power Sources. 2017;357:56-60.

[14] El kharbachi A, Hu Y, Sørby MH, Mæhlen JP, Vullum PE, Fjellvåg H, et al. Reversibility of metal-hydride anodes in all-solid-state lithium secondary battery operating at room temperature. Solid State Ionics. 2018;317:263-7.

[15] Brutti S, Mulas G, Piciollo E, Panero S, Reale P. Magnesium hydride as a high capacity negative electrode for lithium ion batteries. J Mater Chem. 2012;22:14531-7.

[16] Oumellal Y, Zlotea C, Bastide S, Cachet-Vivier C, Leonel E, Sengmany S, et al. Bottom-up preparation of MgH_2 nanoparticles with enhanced cycle life stability during electrochemical conversion in Li-ion batteries. Nanoscale. 2014;6:14459-66.

[17] Huang L, Aymard L, Bonnet J-P. MgH_2-TiH_2 mixture as an anode for lithium-ion batteries: synergic enhancement of the conversion electrode electrochemical performance. J Mater Chem A. 2015;3:15091-6.

[18] Berti N, Cuevas F, Zhang J, Latroche M. Enhanced reversibility of the electrochemical Li conversion reaction with MgH_2–TiH_2 nanocomposites. Int J Hydrogen Energy. 2017;42:22615-21.

[19] Zaïdi W, Oumellal Y, Bonnet JP, Zhang J, Cuevas F, Latroche M, et al. Carboxymethylcellulose and carboxymethylcellulose-formate as binders in MgH_2–carbon composites negative electrode for lithium-ion batteries. J Power Sources. 2011;196:2854-7.

[20] Peng X, Wang H, Hu R, Ouyang L, Liu J, Zhu M. Electrochemical performances of MgH_2 and MgH_2-C films for lithium ion battery anode. J Alloys Compd. 2017;711:473-9.

[21] El kharbachi A, Andersen HF, Sørby MH, Vullum PE, Mæhlen JP, Hauback BC. Morphology effects in MgH_2 anode for lithium ion batteries. Int J Hydrogen Energy. 2017;42:22551-6.

[22] Jangir M, Jain A, Yamaguchi S, Ichikawa T, Lal C, Jain IP. Catalytic effect of TiF_4 in improving hydrogen storage properties of MgH_2. Int J Hydrogen Energy. 2016;41:14178-83.

[23] Kumar S, Jain A, Yamaguchi S, Miyaoka H, Ichikawa T, Mukherjee A, et al. Surface modification of MgH_2 by $ZrCl_4$ to tailor the reversible hydrogen storage performance. Int J Hydrogen Energy. 2017;42:6152-9.

[24] Luo Y, Wang P, Ma L-P, Cheng H-M. Hydrogen sorption kinetics of MgH_2 catalyzed with NbF_5. J Alloys Compd. 2008;453:138-42.

[25] Mulder FM, Singh S, Bolhuis S, Eijt SWH. Extended solubility limits and nanograin refinement in Ti/Zr fluoride-catalyzed MgH_2. J Phys Chem C. 2012;116:2001-12.
[26] Peng B, Xu Y, Wang X, Shi X, Mulder FM. The electrochemical performance of super P carbon black in reversible Li/Na ion uptake. Sci China Phys Mech Astron. 2017;60:064611.
[27] Chen M-L, Oh W-C. Synthesis and highly visible-induced photocatalytic activity of CNT-CdSe composite for methylene blue solution. Nanoscale Res Lett. 2011;6:398.
[28] Gupta V, Saleh TA. Syntheses of carbon nanotube-metal oxides composites; adsorption and photo-degradation. In: Bianco S, editor. Carbon nanotubes - from research to applications. Rijeka: InTech; 2011, p. 295-312.
[29] Haregewoin AM, Wotango AS, Hwang B-J. Electrolyte additives for lithium ion battery electrodes: progress and perspectives. Energy Environ Sci. 2016;9:1955-88.
[30] Schroder K, Alvarado J, Yersak TA, Li J, Dudney N, Webb LJ, et al. The effect of fluoroethylene carbonate as an additive on the solid electrolyte interphase on silicon Lithium-ion electrodes. Chem Mater. 2015;27:5531-42.
[31] Nie M, Demeaux J, Young BT, Heskett DR, Chen Y, Bose A, et al. Effect of Vinylene Carbonate and Fluoroethylene Carbonate on SEI Formation on Graphitic Anodes in Li-Ion Batteries. J Electrochem Soc. 2015;162:A7008-A14.
[32] Grzech A, Lafont U, Magusin PCMM, Mulder FM. Microscopic study of TiF_3 as hydrogen storage catalyst for MgH_2. J Phys Chem C. 2012;116:26027-35.
[33] Li-Ti phase diagram. Factsage thermochemical software and databases, http://www.crct.polymtl.ca/fact/documentation/FTlite/Li-Ti.jpg; [accessed 13 July 2018].
[34] Ganapathy S, Li Z, Anastasaki MS, Basak S, Miao X-F, Goubitz K, et al. Use of nano seed crystals to control peroxide morphology in a nonaqueous Li–O_2 battery. J Phys Chem C. 2016;120:18421-7.

[35] Klein F, Jache B, Bhide A, Adelhelm P. Conversion reactions for sodium-ion batteries. Phys Chem Chem Phys. 2013;15:15876-87.

[36] Ramzan M, Lebègue S, Ahuja R. Transition metal doped MgH_2: A material to potentially combine fuel-cell and battery technologies. Int J Hydrogen Energy. 2010;35:10373-6.